PENSOFT

SENCKENBERG
world of biodiversity

Leibniz Association

A new species of Andean mouse of the genus *Thomasomys* (Cricetidae, Sigmodontinae) from the eastern Andes of Ecuador

Thomas E. Lee Jr.[1], Nicolás Tinoco[2], Jorge Brito[3]

1 *Department of Biology, Abilene Christian University, Abilene, Texas, 79699 USA*

2 *Sección de Mastozoología, Museo de Zoología, Facultad de Ciencias Exactas y Naturales, Pontificia Universidad Católica del Ecuador, Quito, Ecuador*

3 *Instituto Nacional de Biodiversidad (INABIO), Rumipamba 341 y Av. de los Shyris, casilla: 17-07-8976, Quito, Ecuador*

http://zoobank.org/BBDC8B7D-B62B-4AA9-911A-99BE889DE66B

Corresponding author: Thomas E. Lee (leet@acu.edu)

Academic editor Clara Stefen | **Received** 20 November 2021 | **Accepted** 7 March 2022 | **Published** 25 May 2022

Citation: Lee TE Jr,Tinoco N, Brito J (2022) A new species of Andean mouse of the genus *Thomasomys* (Cricetidae, Sigmodontinae) from the eastern Andes of Ecuador. Vertebrate Zoology 72 219–233. https://doi.org/10.3897/vz.72.e78219

Abstract

We name and describe a new species of Andean mouse from the eastern slope of the Andes of central Ecuador (Sangay National Park). This rodent is large-bodied (head-body length 167–184 mm) inhabiting the wet montane forest between 3,400–3,900 m in elevation. A molecular phylogeny based on mitochondrial genes resolved the new species as a member of the "aureus" group, closely related to an undescribed species from north Ecuador. This finding increases the diversity of *Thomasomys* to 48 species, of which 18 species inhabit Ecuador. In addition, the species described herein is the largest species of the genus described in Ecuador.

Key words

Montane forest, Rodentia, Thomasomyini

Introduction

The genus *Thomasomys* contains the highest diversity of any Sigmodontinae genus (Patton et al. 2015; Pardiñas et al. 2017). The genus is mostly confined to the Andes of South America and is usually found above 2,500 m in elevation (Pacheco 2015). Within this genus are members that range in size from *Thomasomys hudsoni* with a head/body length of 88 mm (Brito and Arguero 2016) to *Thomasomys apeco* with head/body length over 235 mm (Gardner and Romo 1993; Ruelas and Pacheco 2021).

The subfamily Sigmodontinae is the most species rich subfamily of Cricetidae (Pardiñas et al. 2017). Sigmodontinae has been the subject of many recent studies concerning both its systematics and what the subfamily can teach us about the last 7 million years of evolutionary and biogeographic history of South America and the Andes in particular (Patton et al. 2015, Pacheco 2015; Brito et al. 2019; Brito et al. 2021; Ruelas and Pacheco 2021).

Currently, 47 species of *Thomasomys* are recognized (Pacheco 2015; Brito et al. 2019; Brito et al. 2021; Ruelas and Pacheco 2021). Internal complexity of *Thomasomys* is high given that it contains, at least, 7 species groups (Pacheco 2003; Salazar-Bravo and Yates 2007; Brito et al. 2019): aureus, baeops, cinereus, gracilis, incanus, macrotis, and notatus. The aureus group contains

the largest-bodied species of the genus, with members ranging from 135 to 238 mm in head-body length, and weighing from 68 to 335 g (Pacheco 2015). Using sequence data from the rapidly evolving cyt *b* gene and a detailed comparative examination of the morphology, we have discovered a previously undocumented taxon within the *T. aureus* group.

Materials and Methods

Studied specimens

We used Sherman traps with an accumulated trap effort of 5,675 trap/nights in very remote and difficult to access mountain regions of Sangay National Park, Ecuador (Lee et al. 2011; and collections by Jorge Brito). We followed the guidelines established by the American Association of Mammalogists (Sikes et al. 2016) for the capture, manipulation and preservation of specimens captured in the field. A qualitative morphological comparison was made based on 60 specimens of the species of the *Thomasomys* that are part of the *T. aureus* group present in Ecuador (Appendix 1). These specimens are deposited in the following collections: Abilene Christian University Natural History Collection (ACUNHC), Abilene, Texas, USA; Museo de Zoología de la Pontificia Universidad Católica del Ecuador, Quito, Ecuador (QCAZ); Escuela Politécnica Nacional, Quito, Ecuador (MEPN), and Instituto Nacional de Biodiversidad, Quito, Ecuador (MECN; formerly known as Museo Ecuatoriano de Ciencias Naturales).

Anatomy, age criteria, and measurements

We followed the main concepts explained by Carleton and Musser (1989), Musser et al. (1998), Pacheco (2003), and Voss (1993) for the description of cranial anatomy. Our description of molar occlusal morphology was based on Reig (1977; upper and lower molars are identified as M/m, respectively). This study followed the terminology and definitions employed by Tribe (1996) and Costa et al. (2011) for age classes and restricted the term adults to those categorized as having molar wear pattern 3 and 4. We obtained the following external measurements in millimeters (mm), some of them registered in the field and reported on specimen tags, others recorded from specimens stored in the museum cabinets: head and body length (HB), tail length (TL), hind foot length (HF, including claw), ear length (E), and body mass (W, in grams (gr). Cranial measurements were obtained with digital calipers, to the nearest 0.01 mm; we employed the following dimensions (see Tribe 1996; Voss 2003; and Musser et al. 1998, for illustrations): condylo-incisive length (CIL), length of upper diastema (LD), crown length of maxillary toothrow (LM), length of incisive foramina (LIF), breadth of incisive foramina (BIF), breadth of rostrum (BR), length of rostrum (LR), length of nasals (LN), length of palatal bridge (LPB), breadth of first maxillary molar (BM1), breadth of bony palate (BBP), least interorbital breadth (LIB), zygomatic breadth (ZB), breadth of zygomatic plate (BZP), orbital fossa length (OFL), braincase breadth (BCB), depth of upper incisor (DI), bular breadth (BB), length of mandible (LMN), crown length of mandibular toothrow (LLM), and length of lower diastema (LLD).

DNA extraction, amplification and sequencing

We extracted DNA from tissues (liver and dry skin) of four specimens identified as *Thomasomys aureus* (MEPN 6144, MECN 2720, MECN 2807, and MECN 5389). All genomic DNA was extracted using the guanidine thiocyanate protocol (Bilton et al. 1996). We amplified the gene cytochrome *b* (cyt *b*) using the forward primer MVZ05 and reverse primers MVZ16H to obtain approximately 500 to 1,000 base pairs. The thermal conditions for PCR are as described in Bonvicino and Moreira (2001).

Phylogenetic analysis

The sequences were edited in Geneious R11.5 (https://www.geneious.com) and aligned with CLUSTALW (Larkin et al. 2007). The evolutionary model for the analysis using Bayesian Inference (BI) and Maximum Likelihood (ML) were obtained using PartitionFinder 2.1 (Lanfear et al. 2016). For the Bayesian and Maximum Likelihood analysis, the best model was 1st position, 2nd position, 3rd position GTR+G+I. The BI analysis was carried out in the MrBayes V3.2 program (Ronquist et al. 2011), the BI analysis consisted of 2 independent runs, each with 4 Markov chains (3 hot and 1 cold); 10 million generations were run, sampling every 1,000 generations. The first 25% of trees were discarded as "burn-in" remaining trees were used to obtain the posterior probabilities (PP). The consensus tree was obtained using the 50% majority rule. Convergence was evaluated by the elective sample size (EES) and the potential scale reduction factor (PSRF). For most of the parameters the EES should be ≥ 200 and for the PSRF most of the values of the parameters should be between 1.0 and 1.2. The ML analysis was carried out in the IQ-Tree program (Trifinopoulos et al. 2016; http://iqtree.cibiv.univie.ac.at). We included 30 sequences from different species of *Thomasomys* from the "aureus" group and some species from other groups of *Thomasomys* (Appendix 2). The genetic distances among species of the "aureus" group were calculated with MEGAX (Kumar et al. 2018), using the Kimura 2-parameter correction model (K-2P) and uncorrected distances (*p*-distances). This allowed a comparison with the genetic distances obtained in other studies of the genus *Thomasomys* (Salazar-Bravo and Yates 2007; Lee et al. 2015, 2018; Brito et al. 2019, 2021; Ruelas and Pacheco 2021).

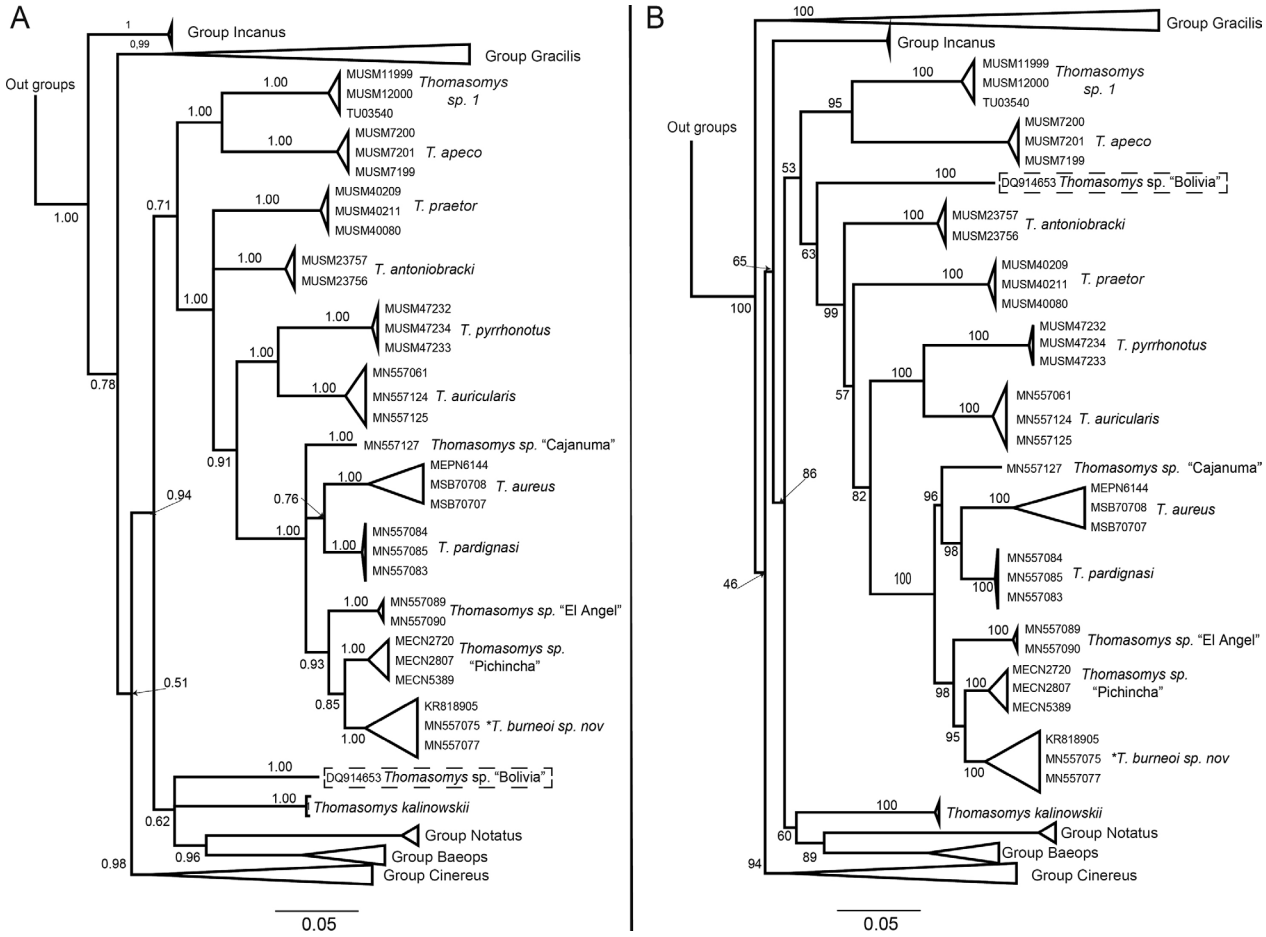

Figure 1. Phylogenetic tree of the species of the group aureus, of the genus *Thomasomys*, based on the mitochondrial gene cytochrome *b* (cyt *b*). **A** Phylogenetic tree of Bayesian inference, the numbers represent the posterior probability values, PP>0.90 are considered high supports. **B** Phylogenetic tree of maximum likelihood, the numbers represent the bootstraps values, BS>70 are considered high supports.

Results

Taxonomic accounts

The IB and ML analysis presented different topologies within the aureus group. The IB analysis failed to recover the monophyly of the aureus group because the sample DQ914653 (*Thomasomys* sp, Bolivia) was located outside the aureus group (Fig. 1A) forming a polytomy (PP=0.62) with other samples: (*Thomasomys* sp. + *Thomasomys kalinowskii* + notatus group + baeops group), while within the aureus group some interspecific relationships could not be resolved (Fig. 1A) [(*Thomasomys* sp.1 PE + *T. apeco*) + (*T. praetor* + *T. antoniobracki* + ((*T. pyrrhonotus* + *T. auricularis*)) + ((*Thomasomys* sp. "Cajanuma" + (*T. aureus* + *T. pardignasi*) + (*Thomasomys* sp. El Angel + (*T.* sp. Pichincha + *Thomasomys* sp. Sangay)))]. In the ML analysis it was possible to recover the monophyly of the aureus group (Fig. 1B), where the main difference was the location of the sample DQ914653, (*Thomasomys* sp.1 Bolivia) and the resolution of the relationships of the samples identified as *T. aureus*. (From different locations in Ecuador). The sample DQ914653 was located within the "aureus" group (BS=99; Fig. 1B): [(*Thomasomys* sp. 1 PE + *T. apeco*) + (*Thomasomys* sp. 1 Bolivia + (*T. antoniobracki* + (((*T. praetor* + (*T. pyrrhomotus* + *T. auricularis*)) + (*T.* sp. Cajanuma + (*T. aureus* + *T. pardignasi*) + (*Thomasomys* sp. El Angel + (*T.* sp. Pichincha + *Thomasomys* sp. Sangay))]. The IB and ML analyzes recovered the samples of *T. pardignasi* and *T. aureus* (all samples), within the same monophyletic clade (1.00/100, Fig. 2) named aureus, this clade presented five internal clades defined and supported (BS>70 / PP>0.90, Fig. 2): *Thomasomys* sp. Cajanuma, *T. aureus*, *T. pardignasi*, *Thomasomys* sp. El Angel, *T.* sp. Pichincha, and *T.* sp. Sangay. Samples of *Thomasomys* sp. El Angel (98/0.93) were located outside the clade formed between *Thomasomys* sp. Pichincha, and *Thomasomys* Sangay (95/0.85, Fig. 2). The genetic variation within the aureus group was 10.68% ± 0.64. While the interspecific variation was from 4% to 14% (Table 1). Within the aureus clade the variation between the internal clades was from 2% to 8% (Table 1).

The data presented in detail below suggest that the taxon discussed represents a new species. We provide below a description of the species, a comparison with other congeners and a discussion of their morphology and phylogenetic relationships. Relevant summaries of qualitative diagnostic traits variation are provided in Table 2 and Fig. 3, respectively.

Table 1. Genetic distance in percentage (K-2P) between the described species of the *Thomasomys aureus* group. The values on the right represent the standard deviation.

Taxa	1	2	3	4	5	6	7	8	9	10	11	12
1 *T. apeco*		1.04	1.12	1.13	1.19	1.05	1.03	1.00	1.30	1.18	1.58	1.57
2 *T.* sp. 1 PE Cusco	10.88		1.00	0.99	1.11	1.12	0.96	1.06	1.14	1.12	1.55	1.50
3 *T. praetor*	11.42	10.99		0.93	0.97	1.05	1.06	1.02	1.09	1.09	1.50	1.19
4 *T. antoniobracki*	10.96	11.09	8.55		0.99	1.04	1.02	0.96	0.85	1.06	1.48	1.33
5 *T. aureus*	12.06	12.24	10.17	10.17		1.14	0.86	0.89	1.38	0.85	1.27	1.14
6 *T. pyrrhonotus*	11.53	12.54	10.37	9.65	9.91		1.02	1.00	1.34	1.09	1.45	1.52
7 *T. burneoi* sp. nov	10.72	12.48	10.41	8.88	4.69	9.47		0.44	1.10	0.72	1.06	1.04
8 *T.* sp. Pichincha	10.93	11.61	10.07	8.66	5.76	9.45	2.15		1.13	0.73	1.02	1.17
9 *T. auricularis*	11.17	11.64	8.42	5.86	9.74	8.15	10.07	8.78		0.81	1.74	1.43
10 *T. pardignasi*	12.49	12.65	10.50	9.06	4.73	10.00	5.26	5.51	7.48		1.14	1.06
11 *T.* sp. El Angel	13.34	12.60	10.53	11.41	7.42	10.77	4.05	4.67	5.45	6.30		1.26
12 *T.* sp. Cajanuma	12.33	12.02	10.20	10.61	6.59	11.23	4.75	5.87	6.85	5.29	7.09	

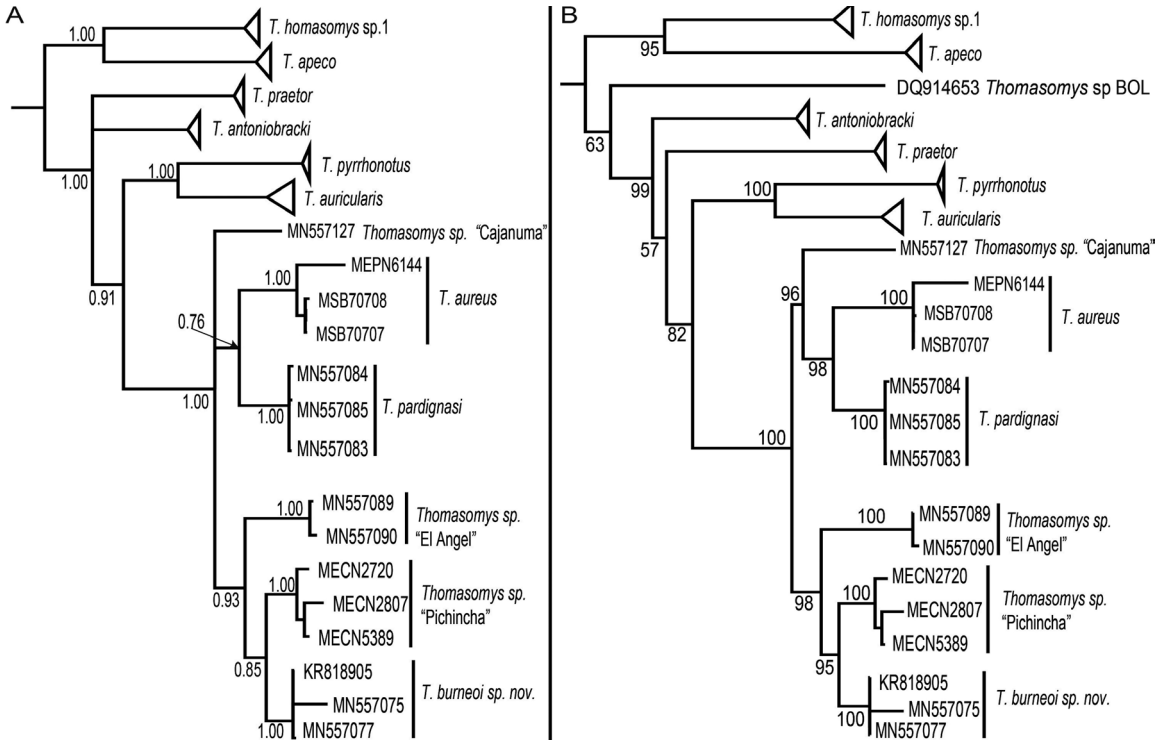

Figure 2. Extension of the clade aureus of the phylogenetic tree of the aureus group. **A** Bayesian inference phylogenetic tree, numbers represent posterior probability values, PP>0.90 are considered high supports. **B** Maximum likelihood phylogenetic tree, numbers represent bootstraps values, BS>70 are considered high supports.

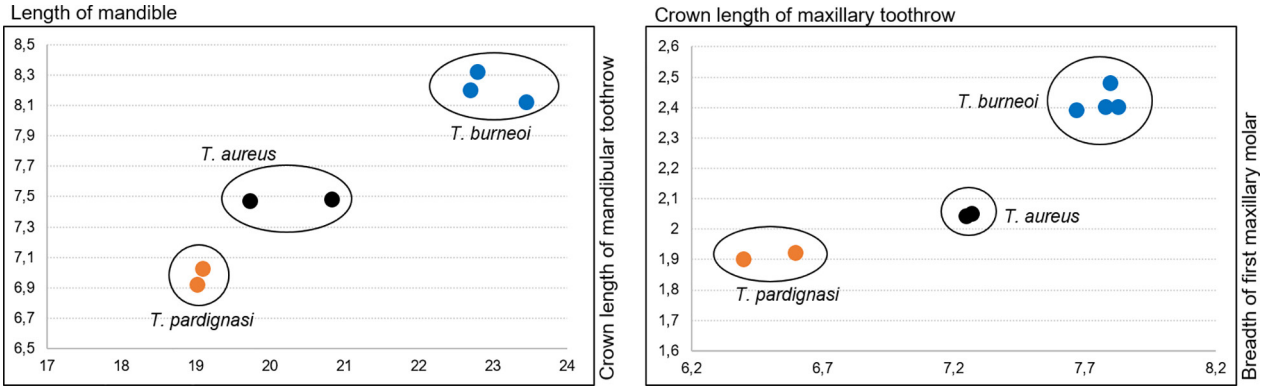

Figure 3. Scatterplots illustrating selected metric comparisons between *Thomasomys burneoi* **sp. nov.**, with *T. aureus* and *T. pardignasi*.

Table 2. Selected morphological differences with species that could be confused with *Thomasomys burneoi* **sp. nov.**, compiled from Pacheco (2015), Brito et al. (2021), and our own observations.

T. burneoi	***T. pardignasi***	***T. aureus* ss**	***T. auricularis***
Head and body length between 167–184 mm	Head and body length between 137–145 mm	Head and body length between 120–173 mm	Head and body length between 138–155 mm
Tail ~ 119–136 % head-body length	Tail ~ 152 % head-body length	Tail ~ 125–141 % head-body length	Tail ~ 122–134 % head-body length
Tail with 12-13 rows of scales per cm on the axis	Tail with 12 rows of scales per cm on the axis	Tail with 16 rows of scales per cm on the axis	Tail with 12 rows of scales per cm on the axis
Genal 1 vibrissae present	Genal 1 and 2 vibrissae present	Genal 1 vibrissae present	Genal 1 vibrissae present
Postauricular patch present	Postauricular patch absent	Postauricular patch absent	Ochraceous postauricular patch present
Body mass > 100 gr.	Body mass < 100 gr.	Body mass < 100 gr.	Body mass < 100 gr.
Upper maxillary row 7.72–8.30 mm	Upper maxillary row 6.4–6.6 mm	Upper maxillary row 6.90–7.42 mm	Upper maxillary row 6.6–7.4 mm
Wide and robust presphenoid	Wide and robust presphenoid	Narrow presphenoid	Narrow presphenoid
Auditory bullae small and inflated	Auditory bullae small and uninflated	Auditory bullae small and uninflated	Auditory bullae large and inflated
Eustachian tube short and wide	Eustachian tube long and narrow	Eustachian tube long and wide	Eustachian tube short and narrow
Moderately developed etmoturbinals	Undeveloped etmoturbinals	Moderately developed etmoturbinals	Moderately developed etmoturbinals
Additional anterior edge on procingulum of M1 present	Additional anterior edge on procingulum of M1 absent	Additional anterior edge on procingulum of M1 absent	Additional anterior edge on procingulum of M1 present
M1 with deep anteroflexus	M1 with shallow anteroflexus	M1 with deep anteroflexus	M1 with deep anteroflexus
M1 with narrow anteroloph	M1 with wide anteroloph	M1 with wide anteroloph	M1 with wide anteroloph
M1-M2 with narrow mesoloph	M1-M2 with wide mesoloph	M1-M2 with wide mesoloph	M1-M2 with wide mesoloph
M3 with distintive mesoloph	M3 with indistinct mesoloph	M3 with indistinct mesoloph	M3 with indistinct mesoloph
m1 with distintive anterolophid	m1 with indistinct anterolophid	m1 with indistinct anterolophid	m1 with distintive anterolophid
Ectolophid present in m1	Ectolophid present in m1 and m2	Ectolophid absent	Ectolophid absent
m1-m2 with ectostylid	m1-m2 lack ectostylid	m1-m2 with ectostylid	m1-m2 with ectostylid
m2-m3 with wide hypoflexid	m2-m3 with narrow hypoflexid	m2-m3 with narrow hypoflexid	m2-m3 with narrow hypoflexid
m3 equals m2	m3 slightly shorter than m2	m3 is longer than m2	m3 equals m2

Taxonomy

Family Cricetidae Fischer, 1817

Subfamily Sigmodontinae Wagner, 1843

Tribe Thomasomyini Steadman & Ray, 1982
Genus *Thomasomys* Coues, 1884

Thomasomys burneoi sp. nov.

Thomasomys praetor: Lee et al. 2011:9; part no *Thomasomys praetor* (Thomas, 1900) *Thomasomys princeps*: Lee et al. 2015:10; part no *Thomasomys princeps* (Thomas, 1895)
Thomasomys aureus: Brito et al. 2019:9; par not *Thomasomys aureus* Tomes, 1860

Burneo's Olfield Mouse
Ratón andino de Burneo (in Spanish)

http://zoobank.org/F47D0CE6-4E92-4712-9E8C-95EA07A859FF

Holotype. MECN 5662 (field number JBM [Jorge Brito Molina] 1812), an adult female captured on August 18, 2017, by Jorge Brito, Jenny Curay, Rocío Vargas and Erika Beltrán, preserved as dry skin, skull, postcranial skeleton, and muscle and liver biopsies in 95% ethanol.

Paratopotype. MECN 5666 (JBM 1822), an adult female collected next to the holotype, on August 18, 2017, by J. Brito, J. Curay, R. Vargas and E. Beltrán.

Paratype. ACUNHC 1548 (field number TEL 2394); 1560 (TEL 2378); QCAZ 11937, adult male captured on July 20, 2010, by Thomas Lee, Carlos Boada, and Amy Scott; QCAZ 11938 (TEL 2295), and adult male captured on July 29, 2010, by TEL at Provincia de Chimborazo, canton Guamote, Parque Nacional Sangay, Lagunas de Atillo –2.17714° S, –78.5075° W, elevation 3,400 m. MECN 5259 (JBM 1409), an adult female collected on October 06, 2016, by J. Brito, R. Vargas, G. Encarnación and J. Velastegui at canton Chambo, Parque Nacional Sangay, Cubillines –1.760633° S, –78.477092° W, elevation 3,900 m.

Type locality. Ecuador, Provincia de Morona Santiago, cantón Morona, parroquia Zúñac, Parque Nacional Sangay

Table. 3. Weight (in grams) and measurements (in millimeters) of adult specimens of *Thomasomys burneoi* **sp. nov.** *T. aureus*. and *T. pardignasi*. Values of *T. aureus* and *T. pardignasi* were taken from Brito et al. (2021). See abbreviations in Material and methods.

	T. burneoi						*T. pardignasi*			*T. aureus*	
Voucher	**ACUNHC 1548**	**ACUNHC 1560**	**MECN 5666**	**MECN 5662**	**MECN 5259**		**MECN 5852**	**MECN 5853**		**MEPN 6144**	**MECN 074**
Sex	M	F	M	F	F		F	F		F	M
Age	5	2	5	3	4		3	3		3	3
HB	183	128	184	172	167		145	137		120	165.5
TL	249	[137]	220	232	207		226	210		183	210.4
HF	42	40	41	43	41		35	38		37	34
E	25	24	28	27	25		23	21		24	23
W	-	-	160	105	111		68	63		72	-
CIL	40.8	32.49	40.13	38.28	39.18		33.1	32.21		32.72	36.57
ZB	22.33	18.78	22.3	22.04	21.81		19.5	19.5		19.28	19.94
LIB	4.78	5.12	5.47	5.16	5.13		5.1	5.33		5.17	5.12
LR	14.52	11.07	13.98	13.14	13.53		11.54	11.31		11.26	12.63
LN	17.41	13.22	16.74	14.53	15.01		13.47	12.27		12.52	15.26
BR	5.88	5.04	8.4	7.91	7.71		5.81	6.24		6.2	6.43
OFL	14.55	11.9	14.17	13.87	13.78		12.22	11.2		12.35	12.33
LD	11.9	8.86	11.94	10.87	10.94		9.1	8.82		8.98	9.94
LM	7.83	7.67	7.72	7.8	7.78		6.4	6.6		7.27	7.25
LIF	9.68	7.48	9.29	8.95	8.64		6.6	6.51		7.04	8.43
BIF	3.47	2.95	3.14	3.13	2.92		2.45	2.37		2.28	2.48
BM1	2.4	2.39	2.19	2.48	2.4		1.9	1.92		2.05	2.04
LPB	6.88	6.26	7.32	6.96	6.88		6.12	6.09		6.61	6.84
BPB	4.75	3.78	3.22	3.34	3.62		2.91	2.96		2.76	2.83
BB	5.65	5.12	5.59	5.43	5.5		4.71	4.87		4.95	5.07
DI	2.39	1.78	2.26	2.05	2.38		1.8	1.79		1.91	2.19
BZP	4.03	3.15	4.08	3.98	3.49		3.27	3.25		3.43	3.73
BCB	16.63	16.39	16.76	17.26	16.31		15.55	15.38		16.22	16.38
LMN	23.45	18.83	23.44	22.7	22.8		19.1	19.03		19.74	20.84
LLM	8.12	8.29	8.19	8.2	8.32		7.02	6.92		7.47	7.48
LLD	5.64	4.79	5.19	5.17	5.03		4.14	4.09		4.58	4.4

Figure 4. *Thomasomys burneoi* **sp. nov.** (MECN 5259, paratype), external appearance of an adult female alive in its natural habitat in the Cubillines, Sangay National Park, Ecuador.

Figure 5. Dry skin in dorsal, ventral, and lateral views of *Thomasomys burneoi*, **sp. nov.** (MECN 5662, holotype). Scale bar = 10 cm.

(Sangay National Park), Laguna Negra –2.179672° S, –78.502919° W (coordinates taken by GPS at the site of collection), elevation 3,553 m).

Diagnosis. A species of *Thomasomys* from the aureus group described by the following character combinations: large size (combined head and body length 167–184 mm); postauricular patch present; wide metatarsal patch; hind foot large > 40 mm; M1 with broad and deep anteroflexus; additional anterior edge on procingulum of M1 present; M3 with metaflexus large and mesoloph distinctive; m1 with small and distinctive anterolophid; m1 with ectolophid; m2–m3 with hypoflexid wide; m3 size equals m2.

Figure 6. Morphology of the dorsal and plantar surface of the right hind foot of: **A**, **C** *Thomasomys burneoi* (MECN 5666, paratype) and *Thomasomys pardignasi* (MECN 5852, holotype) and **B**, **D** Acronyms: I–V = digits, 1–4 = pads, h = hypothenar pad, t = thenar pad. Scales = 10 mm.

Measurements of the holotype (in mm). Head and body length = 172, Tail length = 232, Hind foot length = 43, Ear length = 27, Body mass = 105, Condylo-incisive length = 38.28, Zygomatic breadth = 22.04, Least interorbital breadth = 5.16, Length of rostrum = 13.14, Length of nasals = 14.53, Breadth of rostrum = 7.91, Orbital fossa length = 13.87, Length of upper diastema = 10.87, Crown length of maxillary toothrow = 7.8, Length of incisive foramina = 8.95, Breadth of incisive foramina = 3.13, Breadth of first maxillary molar = 2.84, Length of palatal bridge = 6.96, Breadth of bony palate = 3.34, Bullar breadth = 5.43, Depth of upper incisor = 2.05, Breadth of zygomatic plate = 3.98, Braincase breadth = 17.26, Length of mandible = 22.7, Crown length of mandibular toothrow = 8.2, Length of lower diastema = 5.17. External and craniodental of additional specimens are presented in Table 3.

Morphological description of the holotype and variation. Large body size (head and body length combined with a range between 128 and 184 mm). Cinnamon-brown dorsal fur (Fig. 4, 5), with a faint dark dorsal band; long hairs (medium length on the back = 18–20 mm) dark gray at the base. Light tan dark ventral coat, hairs with (medium length = 10–12 mm) dark gray base, and pale yellowish tips (Fig. 5). Black periocular ring. Postauricular patch present. Mystacial vibrissae long, thick at the base and remain thin towards the tip, exceeding the ear when they are tilted back; 1 superciliary vibrissae present and 1 genal vibrissae present. Ears (between 24–28 mm from notch to margin) externally covered by short orange-brown hairs, pale pink inner surface, dark pale brown margin. Large and wide foot (Fig. 6) with 5 digits ending in thin semi-curved claws. Long white ungueal tufts that slightly exceed the claws. Wide and brown metatarsal patch, that extends to the base of the phalanges. Plantar surface with 6 pads, including 4 interdigitals of similar size to each other (Fig. 6), slightly larger than hypothenar and with very small space between them. Digit I exceeds the base of digit II; digit II and III are the same size and slightly shorter than digit IV; digit V (apparently opposable) reaches the beyond the middle of digit IV. Long tail (207–232 mm; ~127% of HB), ground cinnamon (color 270) and unicolor; square flow scales with three hairs each, which extend over 2.5 to 3 rows of scales in the dorsal basal sector; with 12–13 scales per cm on the shaft. Hirsute tail, even to the rear, hair increasing in length to the apex of the tail. Protuberant anus prominent. Females present six mammary pairs in pectoral, abdominal and inguinal position (sensu Pacheco 2003). The details of soft and genitalia anatomy are unknown.

The cranium is large for the genus (38.2–40.13 mm of CIL). The rostrum is long, somewhat acuminate and narrow, with the nasal bones exceeding the anterior face of the incisors; poorly developed gnathic process (Fig. 7). Posterior margin of the nasal bone slightly exceeds the plane of the lachrymal bone. Moderately deep zygomatic notch (Fig. 8). Small and rounded lacrimal bones. Narrow interorbital region with poorly developed supraorbital ridges, the alveolar maxillary processes well exposed in dorsal view. Supraorbital region with divergent posterior borders (sensu Steppan 1995). Frontoparietal suture V-shaped. Broad and rounded braincase, slightly flattened at the outer edges. Large and concave exoccipital. In the lateral view, small nasolacrimal fissures can be seen in the rostral region and internally, no further development in the ethmoturbinals is distinguishable. Developed and oblique lambdoidal crest. Zygomatic arches sturdy and robust with jugals spanning a short segment of each midarch but distinctly separating zygomatic processes of the maxillary and squamosal bones. Alisphenoid strut wide and robust. Carotid circulatory pattern type 2, derived

Figure 7. Dorsal, ventral and lateral view of the cranium, lateral view of the jaw, occlusal view of the right upper and left lower toothrow of *Thomasomys burneoi* **sp. nov.** (MECN 5662, holotype) from Sangay National Park, Ecuador. Scale = 10 mm.

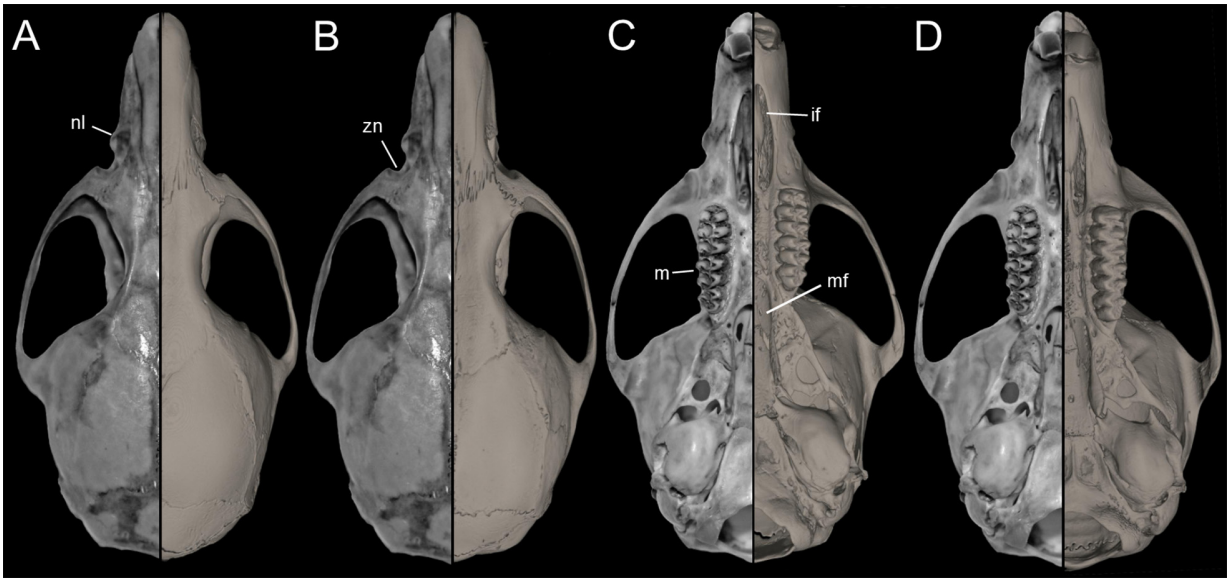

Figure 8. Composed figure illustrating selected differences in the cranial anatomy of *Thomasomys burneoi*, **sp. nov.** (MECN 5662, holotype; left half cranium), *T. pardignasi* (MECN 5852, holotype; right half cranium **A**, **C**, and *T. aureus* sensu stricto (MEPN 6144; right half cranium **B**, **D**. Acronyms: if = incisive foramen, nl = nasolacrimal capsule, m = molars, mf = mesopterygoid fossa, zn = zygomatic notches.

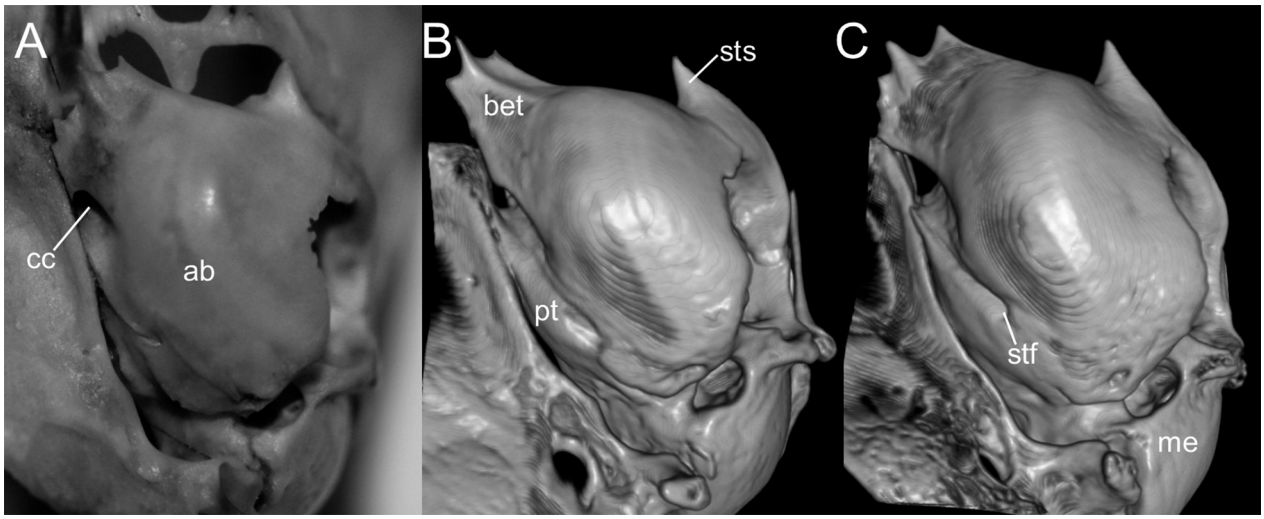

Figure 9. Detail of the bulla in ventral view. **A** *Thomasomys burneoi*, sp. nov. (MECN 5662, holotype), **B** *T. pardignasi* (MECN 5852, holotype), and **C** *T. aureus* sensu stricto (MEPN 6144). Acronyms: ab = auditory bulla, bet = eustachian tube, cc = carotid canal, me = mastoid exposure, pt = petrosal, sts = stapedial process of bulla.

(sensu Voss 1988); carotid canal large (Fig. 9), stapedial foramen and anterior alar fissure small. Postglenoid foramen narrower as the subsquamosal fenestra (Fig. 10); hamular process of squamosal thin, long, but without going beyond the edge on the mastoid capsule. Lightly square tegmen tympanic is superimposed over the suspensory process of the squamous. Lateral expressions of parietals present (Fig. 10); bullae small and inflated; pars flaccida of tympanic membrane present, large; orbicular apophysis of malleus well developed, the manubrium of malleus is blade like with a cup at the distal end. Paraoccipital process large. Hill foramen small; long and narrow incisive foramen with curved edges that subsequently exceed the plane defined by the anterior face of M1 (Fig. 7). Premaxillary capsule slightly widened in the middle and narrow at the ends, maxillary septum of incisive foramen robust and long. Short and narrow palate (sensu Hershkovitz 1962), with the narrow mesopterygoid fossa that enters between the molars reaching the hypoflexus of M3 or 50% of M3, without a medium process. Posterolateral palatal pit small and inconspicuous. Thin and inconspicuous sphenopalatine vacuities covered by the roof of the palate. The basisphenoid is wide, with a small ovale foramen and the middle lacerate foramen is narrow. Auditory bullae small and inflated with short and wide Eustachian tube. Petrosal little exposed (Fig. 9).

Dentary moderately short, robust, with long and wide coronoid process that exceeds the upper edge of the condylar process, (Fig. 9); deep sigmoid notch. Semilunar recess is symmetrical, whose lower edge is wide. Capsular projection of the root of the incisor small.

Opistodont incisors with orange front enamel; brachydont and pentalophodont molars (sensu Hershkovitz 1962). Maxillary molar rows parallel and hypsodont; coronal surfaces crested; main cusps slightly opposite and sloping backwards when viewed from side. The outline of M1 is rectangular with procingulum divided by anteromedian flexus deep into subequal anterolabial and anterolingual conules; additional anterior edge on procingu-

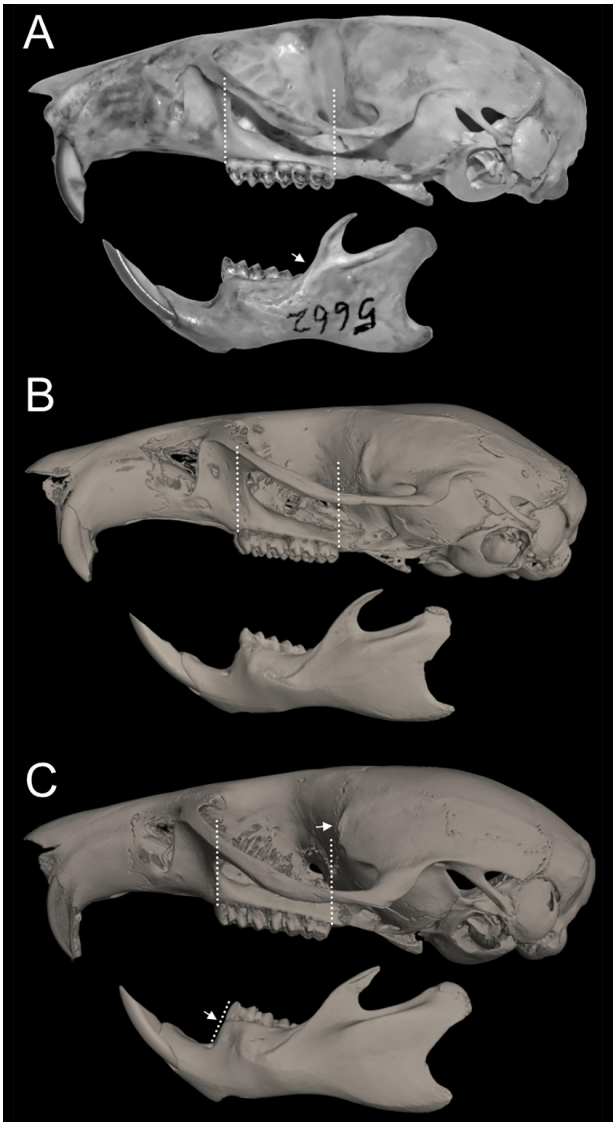

Figure 10. Lateral views of the skulls of: **A** *Thomasomys burneoi* sp. nov. (MECN 5662, holotype), **B** *Thomasomys pardignasi* (MECN 5852, holotype) and **C** *T. aureus* sensu stricto (MEPN 6144).

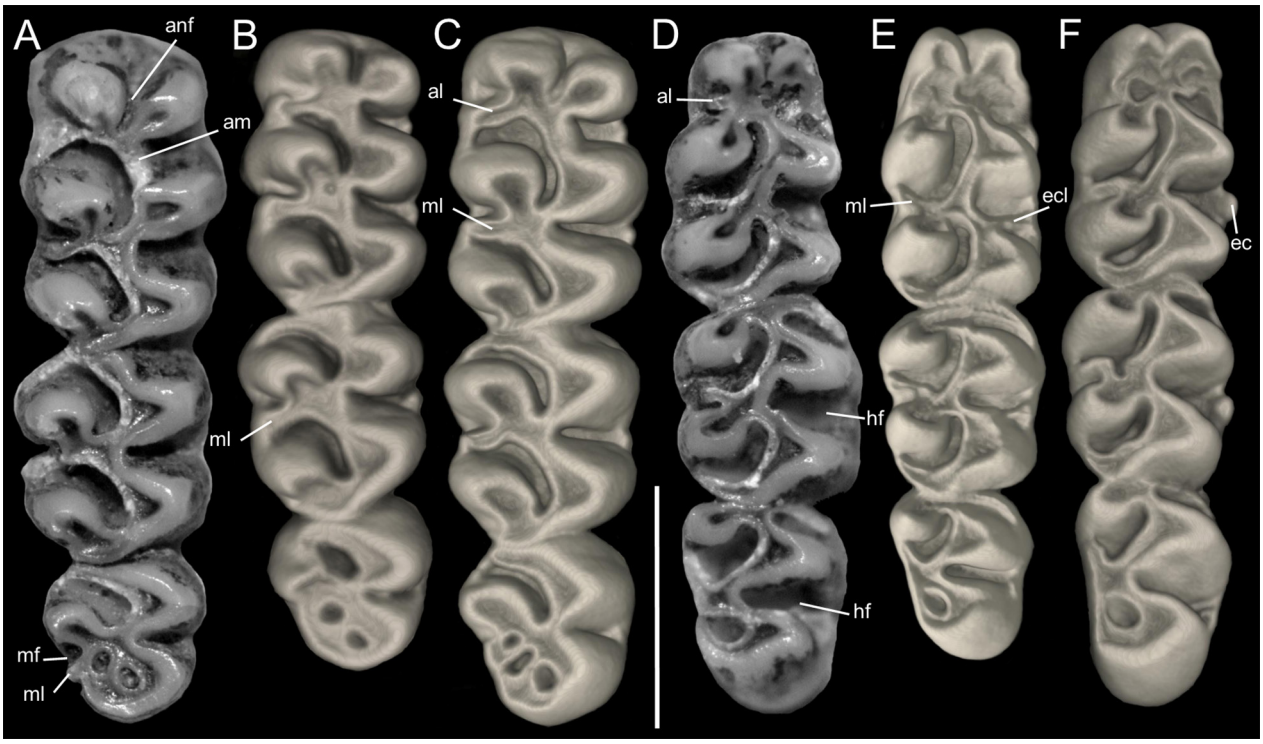

Figure 11. Occlusal view of the right upper (A–C) and right lower (D–F) tooth row of: **A**, **D** *Thomasomys burneoi* sp. nov. (MECN 5662, holotype), **B**, **E** *Thomasomys pardignasi* (MECN 5852, holotype) and **C**, **F** *Thomasomys aureus* (MEPN 6144). Acronyms: anf = anteroflexus, al = anteroloph/id, am = anterior mure, ec = ectostylid, hy = hypoflexid, mf = metaflexus, ml = mesoloph/id, ecl = ectolophid. Scale = 2.5 mm.

lum; narrow anteroloph; narrow mesoloph (Fig 11). M2 is square in outline; mesoloph and posteroloph showing the same condition as in M1. M3 rounded in outline with narrow anteroloph; deep paraflexus; metaflexus large; mesoloph distinctive. Lower molars with main cusps alternated and sloping forward when viewed from side. First lower molar (m1) with anteromedian flexid that divides the procingulum into subequal anterolabial and anterolingual conules; anterolophid distinctive; mesolophid narrow; ectolophid and ectostylid present (Fig. 11). Mesolophid of m2 short and narrow; ectolophid absent and ectostylid present; hypoflexid wide (Fig. 11); m3 equals m2 in size; ectostylid present; hypoflexid wide.

Tuberculum of first rib articulates with transverse processes of seventh cervical and first thoracic vertebrae; second and third thoracic vertebra with differentially elongated neural spine; thoracicolumbar vertebrae 19–20, the 16–17th with moderately developed anapophyses; sacrals 4; caudals 42, with complete hemal arches; 13 ribs present.

Comparisons. *Thomasomys burneoi* **sp. nov.**, apart from being large (Fig. 11; Table 2), differs from *T. pardignasi* Brito et al. (2021) (traits in parentheses) by dorsal uniform color (presenting a dim dark band on the back); back hairs of 18–20 mm (15.53); ventral hairs long, 10–12 mm (9.92 mm); long tail ~127% of HB (~152%); genal vibrissae 2 absent (genal vibrissa 2 absent). Craniodentally, qualitative differences between both species are conspicuous. M1 presents deep anteromedian flexus in *T. burneoi* (shallow); M1–M2 with narrow mesoloph (wide); M3 with distintive mesoloph (indistinct); m1 with ectolophid (present in m1 and m2); m1–m2 with ectostylid (lack ectostylid); m3 equals m2 (m3 is slightly shorter than m2).

Thomasomys burneoi **sp. nov.**, differs from *T. aureus* (based on sensu stricto material, Brito et al. 2021) (traits in parentheses) by tail with 12–13 rows of scales per cm on the axis (16 scales); postauricular patch present (absent). Craniodentally, qualitative differences between both species are conspicuous. Additional anterior edge on procingulum of M1 present in *T. burneoi* (absent); M1 with narrow anteroloph (wide); M3 with distintive mesoloph (indistinct); m1 with distintive anterolophid (indistinct); m1 with ectolophid (absent); m3 equals m2 (m3 is longer than m2). Further comparisons among all the recognized species of *Thomasomys* from the aureus group present in Ecuador are provided in Table 2.

Etymology. Named for Santiago F. Burneo, of the Pontificia Universidad Católica del Ecuador, Quito, Ecuador in recognition of his teaching and support of mammalogists both in Ecuador and the United States of America. The specific epithet is a noun in the genitive case formed by the addition of an "i" to the stem of the name.

Distribution. Known only from Sangay National Park, Chimborazo Province and Morona Santiago Province, Ecuador, 3,400–3,900 m in elevation (Fig. 12).

Natural history. *Thomasomys burneoi* **sp. nov.**, has been recorded in the Altoandino floor (Albuja et al. 2012), in the montane evergreen forest plant formation in the

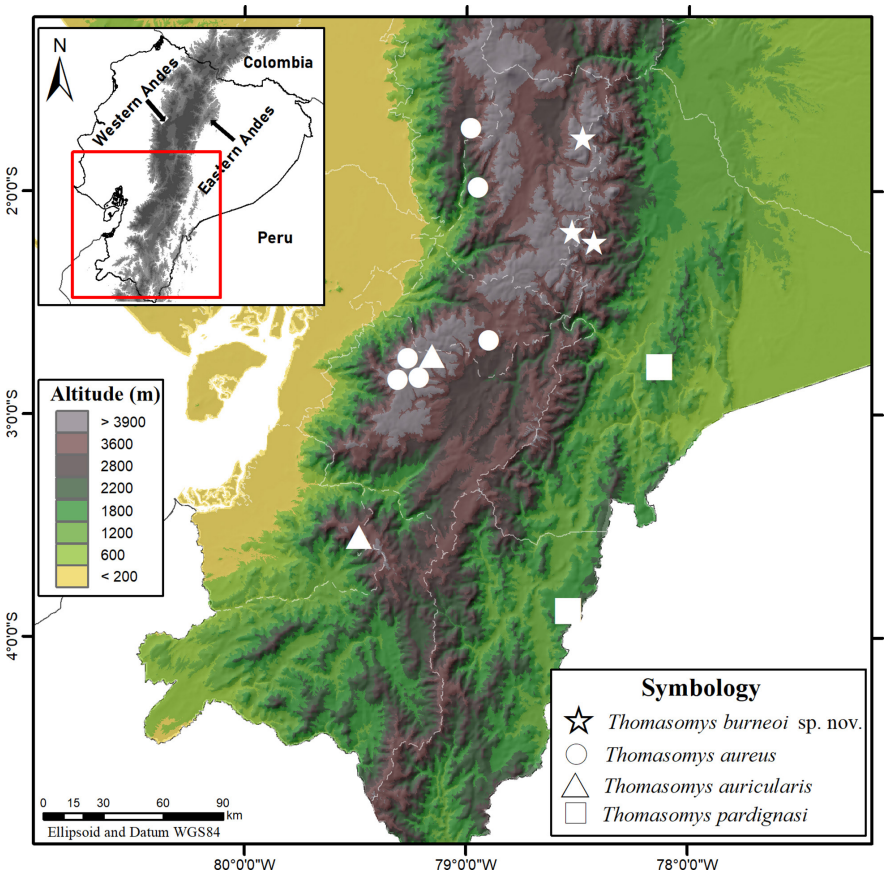

Figure 12. Geographical distribution of *Thomasomys burneoi* sp. nov., and other species of the aureus group in Ecuador. Localities are listed in Appendix 1.

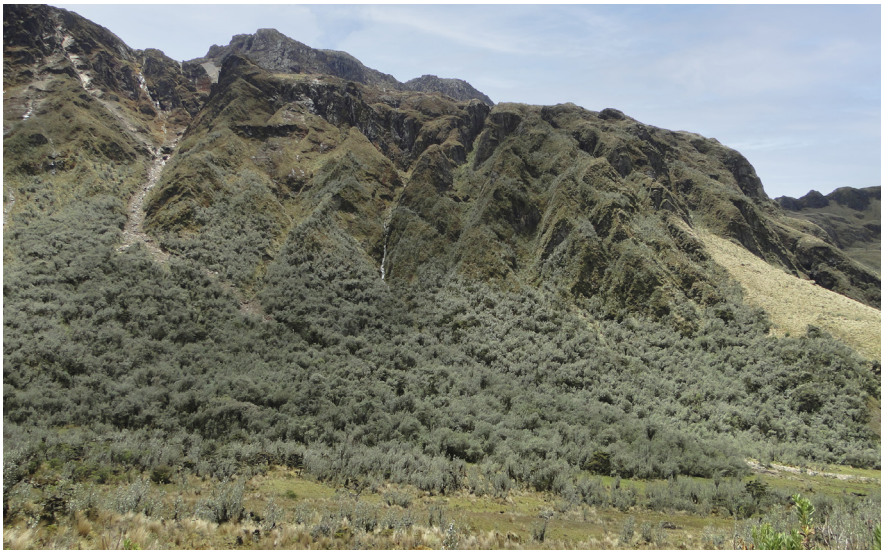

Figure 13. The habitat of a high Andean forest in Cubillines, Sangay National Park where specimens of *Thomasomys burneoi* sp. nov. were found.

southern Cordillera Oriental of the Andes (Ministerio Del Ambiente Del Ecuador 2013). According to the capture data, it is associated with primary elfin forests and páramo (Fig. 13), where the trees are covered by mosses and epiphytes. The specimens were generally collected on thick trunks or branches. In October (dry season), a pregnant female with an embryo was discovered. *Thomasomys burneoi* was found in sympathy with other small mammals *Akodon mollis*, *Caenolestes sangay*, *Cavia patzelti*, *Cryptotis montivagus*, *Microryzomys altissimus*, *M. minutus*, *T. baeops*, *T. cinnameus*, *T. hudsoni*, *T. paramorum* and *T. taczanowskii*.

Discussion

The genus *Thomasomys* evolved into 48 recognized taxa, and most of these species are endemic to the Andes (Pacheco 2015; Brito et al. 2019, 2021; Ruelas and Pacheco 2021; this study). The genus seems to have diverged from a Cricetid ancestor about 6 mya when the Andes were raising to elevations that are conducive to the formation of cloud forests, paramo, and *Polylepis* forest ecosystems (Leite et al. 2014). *Thomasomys* is not common nor does

the genus show great diversity below 2,500 m is elevation (Brito et al. 2021).

Based on molecular data *T. burneoi* falls into the *T. aureus* group (Fig. 1). This finding is not surprising because *T. burneoi* is a large member of the genus *Thomasomys* and shares morphological characters with this group. These characteristics include the large size and the orange-rufous color described above. *Thomasomys burneoi* is sister taxa with some members some of *T. aureus* group (including the recently described *T. pardignasi*) from Pichincha and Carchi Provinces Ecuador (Brito et al. 2021; Fig. 1).

The distribution of *T. burneoi* is poorly known, but we do know that it occurs in Sangay National Park; the elevation where these specimens were collected is around 3,400–3,900 m on the eastern slope of the Andes along the Cordillera Real or Oriental (Fig. 10). The geology of the Lagunas de Atillo is the Tarqui Formation that consists of rhyodacitic pyroclastics and lavas (Longo and Baldock 1982). The type and paratypes were caught in a heterogenous habitat of mixed páramo and temperate forests (Fig. 11). The páramo component consisted of grasses (*Stipa ichu*), Asteraceae, and Bromeliaceae (*Puya*). The forests were dominated by *Polylepis* trees and plants of the families Calceolariaceae, Passifloraceae, Fabaceae, Onagraceae, Orchidaceae, Polypodiaceae (ferns), and Valerianaceae (Lee et al. 2011). Poorly drained areas of the paramo had thick beds of mosses. These animals were caught on steep slopes or at the base of rock cliffs (Fig. 11). All of these habitats are in the vicinity of the Lagunas de Atillo and Cubillines which are deep, cold, oligotrophic, lakes with marshes of reeds along parts of their banks. In addition, we managed to acquirer specimens of *Amblyopinus colombiae* which are beetles that were found living on the skin of *T. burneoi* usually on the dorsum of the neck (Lee et al. 2011).

Recent expeditions to previously unexplored areas in Sangay National Park have resulted in the discovery of sanctuaries of diversity, from which numerous species new to science have been described (eg, Ojala-Barbour et al. 2013; Brito et al. 2017a, b; Páez and Ron et al. 2019). During the eighteen expeditions made to Sangay National Park (2009–2018), and despite the extreme logistical difficulties, it was possible to collect around 1,000 samples of mammals from ca. 120 taxa (Lee et al. 2011; Brito and Ojala-Barbour 2016; Brito in prep.), three of which were described as new (*Caenolestes sangay* Ojala-Barbour et al. (2013), *Rhipidomys albujai* Brito et al. (2017), and *Thomasomys salazari* Brito et al. (2019)) an additional four are also possibly new to science. *Thomasomys burneoi* **sp. nov.** is just one example of the still overlooked Ecuadorian diversity.

Conflict of Interest

The authors declare no conflict of interest.

Acknowledgements

We thank the staff of the Ministry of Environment of Morona Santiago, especially Paúl Tito and Christian Clavijo, for their collaboration with logistic help in the field. Furthermore, we thank Glenda Pozo, Jenny Curay, Rocío Vargas, Érika Beltrán and Eulogio Zúñiga for their assistance during the work collecting specimens. Jorge Brito thanks Earth Deeds Carbon Mitigation Initiative of Pacific Lutheran University for the funds allocated to carry out part of the expeditions, and Diego Inclán, Francisco Prieto of INABIO for their sponsorship and permanent support. Tom Lee thanks the Clark Stevens endowment for funding work on this project. Mateo Vega kindly assisted in preparing Figure 12. The Ministry of the Environment of Ecuador granted the respective permits to Tom Lee and Jorge Brito for the collection of specimens in Sangay National Park: No. 02-2010-FAU-DPAP-MA, and No. 007-IC-DPACH-MAE-2016.

References

Albuja L, Almendáriz A, Barriga R, Montalvo LD, Cáceres F, Román JL (2012) Fauna de vertebrados del Ecuador. Escuela Politécnica Nacional, Quito.

Bilton DT, Jaarola M (1996) Isolation and purification of vertebrate DNAs. In Clapp JP, (Ed) Species diagnostics protocols: PCR and other nucleic acid methods in molecular biology Humana Press. Totowa, New Jersey, 25–37.

Bonvicino CR, Moreira MA (2001) Molecular phylogeny of the genus *Oryzomys* (Rodentia: Sigmodontinae) based on cytochrome *b* DNA sequences. Molecular Phylogenetics and Evolution 18: 282–292.

Brito J, Arguero A (2016) Nuevas localidades para tres especies de mamíferos pequeños (Rodentia: Cricetidae) escasamente conocidos en Ecuador. Mastozoología Neotropical 2: 521–527.

Brito J, Ojala-Barbour R (2016) Mamíferos no voladores del Parque Nacional Sangay, Ecuador. Papéis Avulsos de Zoologia 56: 45–61. http://dx.doi.org/10.1590/0031-1049.2016.56.05

Brito J, Batallas D, Yánez-Muñoz MH (2017) Ranas terrestres *Pristimantis* (Anura: Craugastoridae) de los bosques montanos del río Uáano, Ecuador: Lista anotada, patrones de diversidad y descripción de cuatro especies nuevas, Neotropical Biodiversity 3: 125–156. https://doi.org/10.1080/23766808.2017.1299529

Brito J, Tinoco N, Chávez D, Moreno-Cárdenas P, Batallas D, Ojala-Barbour R (2017) New species of arboreal rat of the genus *Rhipidomys* (Cricetidae, Sigmodontinae) from Sangay National Park, Ecuador. Neotropical Biodiversity 3: 65–79. https://doi.org/10.1080/23766808.2017.1292755

Brito J, Tinoco N, Curay J, Vargas R, Reyes-Puig C, Romero V, Pardiñas UF (2019) Diversidad insospechada en los Andes de Ecuador: filogenia del grupo "cinereus" de *Thomasomys* y descripción de una nueva especie (Rodentia, Cricetidae). Mastozoología Neotropical 26: 308–330. https://doi.org/10.31687/saremMN.19.26.2.0.04

Brito J, Vaca-Puente S, Koch C, Tinoco N (2021) Discovery of the first Amazonian *Thomasomys* (Rodentia, Cricetidae, Sigmodontinae): a new species from the remote Cordilleras del Cóndor and Kutukú in Ecuador. Journal of Mammalogy 102: 615–635. https://doi.org/10.1093/jmammal/gyaa183

Carleton MD, Musser CG (1989) Systematic studies of Oryzomyine rodents (Muridae, Sigmodontinae): A synopsis of *Microryzomys*. Bulletin of the American Museum of Natural History 191: 1–83.

Costa BMA, Geise L, Pereira LG, Costa LP (2011) Phylogeography of *Rhipidomys* (Rodentia: Cricetidae: Sigmodontinae) and description of two new species from southeastern Brazil. Journal of Mammalogy 92: 945–962. https://doi.org/10.1644/10-MAMM-A-249.1

Fischer G (1817) Adversaria zoologica. Fasciculus primus. Quaedam ad Mammalium systema et genera illustranda. Mémoires de la Société impériale des naturalistes de Moscou 5: 357– 446, 2 pls.

Gardner AL, Romo M (1993) A new *Thomasomys* (Mammalia: Rodentia) from the Peruvian Andes. Proceedings of the Biological Society of Washington 106: 762–774.

Hershkovitz P (1962) Evolution of Neotropical cricetine rodents (Muridae) with special reference to the phyllotine group. Fieldiana Zoology 46: 1–524.

Kumar S, Stecher G, Li M, Knyaz C, Tamura K (2018) MEGA X: Molecular Evolutionary Genetics Analysis across computing platforms. Molecular Biology and Evolution 35: 1547–1549. https//doi/10.1093/molbev/msy096

Lanfear R, Frandsen PB, Wright M, Senfeld T, Calcott B (2016) PartitionFinder 2: new methods for selecting partitioned models of evolution for molecular and morphological phylogenetic analyses. Molecular Biology and Evolution 34: 772–773. https://doi.org/10.1093/molbev/msw260

Larkin MA, Blackshields G, Brown NP, Chenna R, McGettigan PA, McWilliam H, Valentin F, Wallace IM, Wilm A, Lopez R, Thompson JD, Gibson TJ, Higgins DG (2007) Clustal W and clustal X version 2.0. Bioinformatics 23: 2947–2948. https://doi.org/10.1093/bioinformatics/btm404

Lee TE Jr, Boada-Terán C, Scott AM, Burneo SF, Hanson JD (2011) Small mammals of Sangay National Park, Chimborazo Province and Morona Santiago Province, Ecuador. Occasional Papers, Museum of Texas Tech University. 305: 1–16.

Lee TE Jr, Ritchie AR, Vaca-Puente S, Brokaw JM, Camacho MA, Burneo SF (2015) Small mammals of Guandera Biological Reserve, Carchi Province, Ecuador and comparative Andean small mammal ecology. Occasional Papers, Museum of Texas Tech University 334: 1–17.

Lee TE Jr, Tinoco N, Feller MJ, Gomez D, Hanson JD, Camacho MA, Burneo SF (2018) Mammals of Yacuri National Park, Loja, Province, Ecuador. Occasional Papers, Museum of Texas Tech University 357: 1–17.

Leite RN, Kolokotronis SO, Almeida FC, Werneck FP, Rogers DS, Weksler M (2014) In the wake of invasion: tracing the historical biogeography of the South American cricetid radiation (Rodentia, Sigmodontinae). PLoS One 9: e100687.

Longo R, Baldock JW (1982) National Geological Map of the Republic of Ecuador. Ministerio de Recursos Naturales Energeticos, Quito.

Ministerio del Ambiente del Ecuador (2013) Sistema de Clasificación de los Ecosistemas del Ecuador Continental. Subsecretaría de Patrimonio Natural, Quito.

Musser GG, Carleton MD, Brothers E, Gardner AL (1998) Systematic studies of oryzomyine rodents (Muridae, Sigmodontinae): diagnoses and distributions of species formerly assigned to *Oryzomys capito*. Bulletin of the American Museum of Natural History 236: 1–376.

Ojala-Barbour R, Pinto CM, Brito J, Albuja VL, Lee Jr TE, Patterson BD (2013) A new species of shrew-opossum (Paucituberculata: Caenolestidae) with a phylogeny of extant caenolestids. Journal of Mammalogy 94: 967-982. https://doi.org/10.1644/13-MAMM-A-018.1

Pacheco V (2003) Phylogenetic analysis of the Thomasomyini (Muroidea: Sigmodontinae) based on morphological data. Ph.D. Dissertation, University of New York, NY.

Pacheco V (2015) Genus *Thomasomys* Coues, 1884. In: Patton JL, Pardiñas UFJ, D´Elia G (Eds) Mammals of South America, Vol. 2: Rodents University of Chicago Press, Chicago, IL, 617–682.

Pacheco V (2021) Range extension of *Thomasomys princeps* (Thomas, 1895) (Rodentia, Sigmodontinae) and first record in Venezuela. Check List 17: 385–393. https://doi.org/10.15560/17.2.3

Páez NB, Ron SR (2019) Systematics of *Huicundomantis*, a new subgenus of *Pristimantis* (Anura, Strabomantidae) with extraordinary cryptic diversity and eleven new species. ZooKeys 868, 1–112. https://www.doi.org/10.3897/zookeys.868.26766

Pardiñas UFJ, Ruelas D, Brito J, Bradley LC, Bradley RD, Garza NO, Krystufek B, Cook JA, Soto EC, Salazar-Bravo J, Shenbrot GI, Chiquito EA, Percequillo AR, Prado JR, Haslauer R, Patton JL, Leon-Paniagua L (2017) Cricetidae (true hamsters, voles, lemmings and new world rats and mice)–species accounts of Cricetidae. In: Wilson DE, Lacher TE Jr, Mittermeier RA (Eds) Handbook of the mammals of the world. Rodents II 7 (2017): 280–535.

Patton JL, Pardiñas UFJ, D'Elía G (2015) Mammals of South America, Vol. 2: Rodents. University of Chicago Press, Chicago, IL.

Reig OA (1977) A proposed unified nomenclature for the enameled components of the molar teeth of the Cricetidae (Rodentia). Journal of Zoology 181: 227–241.

Ronquist F, Teslenko M, Van Der Mark P, Ayres D, Darling AA, Höhna S, Larget B, Liu L, Suchard MA, Huelsenbeck JP (2011) MrBayes 3.2: efficient Bayesian phylogenetic inference and model choice across a large model space. Systematic Biology 61: 539–542. https://doi.org/10.1093/sysbio/sys029

Ruelas D, Pacheco V (2021) A new species of *Thomasomys* Coues, 1884 (Rodentia: Sigmodontinae) from the montane forests of northern Peru with comments on the "aureus" group. Revista peruana de biología 28: e19912. http://dx.doi.org/10.15381/rpb.v28i3.19912

Salazar-Bravo J, Yates TL (2007) A new species of *Thomasomys* (Cricetidae: Sigmodontinae) from central Bolivia. In: The quintessential naturalist: Honoring the life and legacy of Oliver P. Pearson. University of California Publications in Zoology Berkeley, 747–774.

Sikes RS, the Animal Care and Use Committee of the American Society of Mammalogists (2016) Guidelines of the American Society of Mammalogists for the use of wild mammals in research and education. Journal of Mammalogy 97: 663–688. https://doi.org/10.1093/jmammal/gyw078

Steadman D, Ray C (1982) The relationships of *Megaoryzomys curioi*, and extinct cricetine rodent (Muroidea: Muridae) from the Galápagos Islands, Ecuador. Smithsonian Contributions to Paleobiology 51: 1–23.

Steppan S (1995) Revision of the tribe Phyllotini (Rodentia: Sigmodontinae), with a phylogenetic hypothesis for the Sigmodontinae. Fieldiana Zoology 1464: 1–112.

Thomas O (1895) On small mammals from Nicaragua and Bogota. Annals and Magazine of Natural History, Series 6, 16: 55–60.

Thomas O (1900) Descriptions of two new murines from Peru and a new hare from Venezuela. Annals and Magazine of Natural History, Series 7, 5: 354–357.

Tomes RF (1860) Notes on a collection of mammals made by Mr. Fraser in the Republic of Ecuador. Proceedings of the Zoological Society of London 1860 (part II): 211–221.

Tribe CJ (1996) The neotropical rodent genus *Rhipidomys* (Cricetidae: Sigmodontinae): a taxonomic revision. Ph.D. Dissertation, University College London. London.

Trifinopoulos J, Nguyen LT, Von Haeseler A, Minh A (2016) W-IQ-TREE: a fast online phylogenetic tool for maximum likelihood analysis. Nucleic Acids Research 44: W232–W235. https://doi.org/10.1093/nar/gkw256

Voss RS (1988) Systematics and ecology of ichthyomyine rodents (Muroidea): patterns of morphological evolution in a small adaptive radiation. Bulletin of the American Museum of Natural History 188: 262–493.

Voss RS (1993) A revision of the Brazilian muroid rodent genus *Delomys* with remarks on "Thomasomyine" characters. American Museum Novitates 3073: 1–44.

Voss RS (2003) A new species of *Thomasomys* (Rodentia: Muridae) from Eastern Ecuador, with remarks on mammalian diversity and biogeography in the Cordillera Oriental. American Museum Novitates 3421: 1–47.

Wagner JA (1843) Die Säugthiere in Abbildungen nach der Natur mit Beschreibungen von Dr. Johann Christian Daniel von Schreber. Supplementband. Dritter Abtheilung: Die Beutelthiere und Nager (erster Abschnitt). Erlangen (Expedition das Schreber'schen Säugthier- und des Esper'sschen Schmetterlingswerkes, und in Commission der Voss'schen Buchhandlung in Leipzig), 3: i–xiv + 1–614, pl. 85–165. https://doi.org/10.5962/bhl.title.67399

Appendix I

Thomasomys sp. Pichincha (n=22). **Pichincha**, Lloa, Atacazo: MECN 2711 (0°18′26.996″ S, 78°40′52.855″ W, 2,743 m), Solaya River: MECN 2720–21 (0°1′45.040″ S, 78°49′4.0872″ W, 2,527 m), Nono, Río Verde Cocha: MECN 2807 (0°,7′39.939″ S, 78°35′28.640″ W, 3,562 m); Reserva Geobotánica Pululahua: MECN 5053, 5208 (0°1′12.9″ N, 78°29′35.29″ W, 3,190 m); Mejía, Tambillo Alto: MECN 5389 (0°24′26.607″ S, 78°33′57.563″, 2,789 m). **Cotopaxi**, Reserva Integral Otonga: QCAZ 2406 (0°25′8.04″ S, 79°0′14.04″ W, 2,000 m). *Thomasomys* sp. Cajanuma (n=1). Loja, Cajanuma, Parque Nacional Podocarpus: MECN (6369). *Thomasomys* sp. "El Ángel" (n=14). **Carchi**, La Libertad, Bosque de Polylepis: MECN 3716, 3729, 3746–47, 4374–75, MEPN 10486, 10645–46, 10774, 10871, 11706 (0°42′43.927″ N 77°58′53.90″ W, 3,600 m). *Thomasomys aureus* "Cajanuma" (n=1). **Loja**, Cajanuma, Parque Nacional Podocarpus: MN557127 (4°6′59.90″ S, 79°10′21.176″ W, 2,790 m). *Thomasomys* cf. *T. aureus* "Shucos" (n=1). **Zamora Chinchipe**, Shucos: QCAZ 13243 (3°49′14.987″ S, 79°7′2.8626″ W, 2,923 m).

Thomasomys aureus (n=6). **Azuay**, Molleturo: MECN 74 (2°49′0.0114″ S, 79°13′0.12″ W, 2,700 m), Mazan: MEPN 11090 (2°35′42″ S, 78°33′48.999″ W, 2,900 m), Laguna Toreadora: QCAZ 6011 (2°46′48.828″ S, 79°13′25.319″ W, 3,920 m), Molleturo: MEPN 10008 (2°50′5.9994″ S, 79°22′26.399″ W, 3,600 m). **Bolívar**, Cruz de Lizo, Tatahuazo River: MECN 6144 (1°43′11.99″ S, 79°0′0.00″ W, 2,600 m). **Cañar**, Nazón: MEPN 6143 (2°40′11.99″ S, 78°,54′0″ W, 3,050 m). *Thomasomys auricularis* (n=7). **Azuay**, Molleturo, Luspa: MECN 71 (2°48′43.963″ S, 79°16′4.5618″ W, 3,700 m), Laguna Toreadora: MECN 72, MZUA 197, QCAZ 6011, 6015 (2°46′0.5988″ S, 79°13′23.041″ W, 4,000 m). **El Oro**, Salvias, Cerro de Arcos: MECN 4686, 4696 (3°33′10.464″ S, 79°29′3.822″ W, 3,500 m). *Thomasomys burneoi* **sp. nov.** (n=5). **Chimborazo**, Chambo, Parque Nacional Sangay, Cubillines: MECN 5259 (1°45′38.278″ S, 78°28′37.530″ W, 3,900 m). **Morona Santiago**, Morona, Parque Nacional Sangay, Atillo: MECN 5662, 5666, QCAZ 11939–40 (2°10′46.819″ S, 78°30′10.508″ W, 3,553 m). *Thomasomys pardignasi* (n=3). **Morona Santiago**, Cordillera de Kutukú: MECN 5852-53 (2°47′13.992″ S, 78°7′53.975″ W, 2,215 m). **Zamora Chinchipe**, Río Blanco, Cordillera del Cóndor: MEPN 12053 (3°53′59.999″ S, 78°30′54″ W, 1,750 m).

Appendix II

We included 30 sequences from different species of *Thomasomys* from the "aureus" group and some species from other groups of *Thomasomys*:

Accession Number	Identification
AF108679	*Chilomys intans*
KY366342	*Rhipidomys albujai*
KY366344	*Rhipidomys albujai*
HM594636	*Rhipidomys emiliae*
HM594628	*Rhipidomys ipukensis*
HM594659	*Rhipidomys leucodactylus*
HM594646	*Rhipidomys macrurus*
HM594643	*Rhipidomys mastacalis*

Accession Number	Identification
HQ634184	*Rhipidomys wetzeli*
MN557094	*Thomasomys paramorum*
MN557095	*Thomasomys paramorum*
MN557096	*Thomasomys paramorum*
MN557097	*Thomasomys paramorum*
MN557098	*Thomasomys paramorum*
DQ914643	*Thomasomys andersoni*
DQ914644	*Thomasomys andersoni*

Accession Number	Identification
MW788413	*Thomasomys antoniobracki*
MW788412	*Thomasomys antoniobracki*
MW788416	*Thomasomys apeco*
MW788414	*Thomasomys apeco*
MW788415	*Thomasomys apeco*
MW788418	*Thomasomys aureus*
MW788417	*Thomasomys aureus*
MN557061	*Thomasomys auricularis*
MN557124	*Thomasomys auricularis*
MN557125	*Thomasomys auricularis*
DQ914645	*Thomasomys australis*
DQ914650	*Thomasomys australis*
KR818876	*Thomasomys baeops*
KR818877	*Thomasomys baeops*
KR818878	*Thomasomys baeops*
MN557062	*Thomasomys bombycinus*
KR818905	*Thomasomys burneoi* sp. nov
MN557075	*Thomasomys burneoi* sp. nov
MN557077	*Thomasomys burneoi* sp. nov
DQ914648	*Thomasomys caudivarius*
MN557059	*Thomasomys caudivarius*
MN557060	*Thomasomys caudivarius*
MN557126	*Thomasomys caudivarius*
KR818895	*Thomasomys cinnameus*
KR818896	*Thomasomys cinnameus*
KR818897	*Thomasomys cinnameus*
AF108673	*Thomasomys daphne*
DQ914649	*Thomasomys daphne*
KY754167	*Thomasomys daphne*
EU579476	*Thomasomys erro*
KR818901	*Thomasomys fumeus*
AF108674	*Thomasomys gracilis*
MN557076	*Thomasomys hudsoni*
MN557078	*Thomasomys hudsoni*
MN557079	*Thomasomys hudsoni*
AF108675	*Thomasomys ischyurus*
AF108678	*Thomasomys kalinowskii*
DQ914647	*Thomasomys ladewi*
DQ914652	*Thomasomys ladewi*
AF108676	*Thomasomys notatus*
AF108677	*Thomasomys oreas*

Accession Number	Identification
MN557083	*Thomasomys pardignasi*
MN557084	*Thomasomys pardignasi*
MN557085	*Thomasomys pardignasi*
MW788421	*Thomasomys praetor*
MW788419	*Thomasomys praetor*
MW788420	*Thomasomys praetor*
MW788424	*Thomasomys pyrrhonotus*
MW788423	*Thomasomys pyrrhonotus*
MW788422	*Thomasomys pyrrhonotus*
KR818888	*Thomasomys salazari*
KR818889	*Thomasomys salazari*
KR818890	*Thomasomys salazari*
KR818900	*Thomasomys silvestris*
MN557063	*Thomasomys silvestris*
MN557064	*Thomasomys silvestris*
MW788426	*Thomasomys* sp. 1 sensu Pacheco (2003)
MW788425	*Thomasomys* sp. 1 sensu Pacheco (2003)
DQ914653	*Thomasomys* sp. 1 sensu Pacheco (2003)
MN557127	*Thomasomys* sp. Cajanuma
MN557089	*Thomasomys* sp. El Angel
MN557090	*Thomasomys* sp. El Angel
KR818879	*Thomasomys taczanowskii*
KR818880	*Thomasomys taczanowskii*
KR818881	*Thomasomys taczanowskii*
KR818882	*Thomasomys taczanowskii*
KR818883	*Thomasomys taczanowskii*
KR818884	*Thomasomys taczanowskii*
KR818885	*Thomasomys taczanowskii*
KR818886	*Thomasomys taczanowskii*
KR818887	*Thomasomys taczanowskii*
MN557069	*Thomasomys taczanowskii*
MN557070	*Thomasomys taczanowskii*
MN557071	*Thomasomys taczanowskii*
MN557086	*Thomasomys taczanowskii*
KR818898	*Thomasomys ucucha*
KR818899	*Thomasomys ucucha*
MN557093	*Thomasomys ucucha*
KR818902	*Thomasomys vulcani*
KR818903	*Thomasomys vulcani*
KR818904	*Thomasomys vulcani*